

Steel cleanliness and hydrogen in liquid steel

R. DEKKERS*, B. BLANPAIN*, J. PLESSERS†, and P. WOLLANTS*

*K.U.leuven, Department of Metallurgy and Materials Engineering, Heverlee, Belgium

†Heraeus Electro-Nite Int., Houthalen, Belgium

The feasibility of using hydrogen to obtain clean steels is investigated. High hydrogen contents are generally considered as detrimental due to the risk of flakes, bubbles and breakouts during casting. Hydrogen can nonetheless be removed by degassing of the steel. The results of industrial campaigns, where total oxygen content and hydrogen content were monitored, are presented. High resolution microscopy of inclusions and laboratory experiments on the rate of inclusion removal by CaO-Al₂O₃ slags at different partial hydrogen have been carried out. So far, evidence that hydrogen may influence inclusions or the steel cleanliness is not clear.

Keywords: hydrogen, cleanliness, inclusions.

Introduction

With increasing demands on steel quality, control of parameters affecting the steel cleanliness becomes more important. Steel cleanliness may refer to the number of impurity elements or the number of inclusions present in the steel. The number, morphology and type of non-metallic inclusions determine the steel cleanliness. In industry, the total amount of oxygen in steel is frequently used to indicate the degree of steel cleanliness. Since the amount of dissolved oxygen is about constant, the total oxygen content is a measure of the number of oxide inclusions in the steel. Non-metallic inclusions primarily result from the deoxidation of the steel. Deoxidation occurs by the addition of a strong deoxidizer, typically aluminium, and is necessary to prevent the formation of carbon monoxide bubbles during casting of the steel. The presence of inclusions may have a detrimental effect on the product quality. It also increases the production cost. Internal cleanliness is currently the topic in steel production with the largest impact on competitiveness.

In this paper, the results of an industrial-academic project are given. The project aims to evaluate the possibilities of process adaptations based on hydrogen control. Therefore, investigation of the effect of hydrogen on the formation and separation of inclusions is required. Both industrial and experimental measurements are considered.

Multiple sources of hydrogen in steelmaking have been identified. In particular, moisture from refractory materials, and from additions for deoxidation and alloying have been found to increase the hydrogen content of the steel¹. The hydrophilic calcium oxide in the slag² and decomposition of refractory binders^{3,4}, which are required for sufficient thermal shock resistance, also account for hydrogen entering into the steel. A large amount of industrial research focuses on the removal of hydrogen during the degassing of the steel^{1,3-8}. Vacuum favours the formation of gas bubbles, which contain a mixture of carbon monoxide, nitrogen and hydrogen. Because of their low density, gas bubbles easily float to the steel surface where they separate from the steel bath. Hydrogen critical steel grades are therefore always produced via a degassing stage. Argon bubbling also enhances the process of hydrogen removal because it decreases the partial hydrogen pressure^{3,6}.

Commonly, problems of hydrogen in steel are related to the formation of flakes, the occurrence of break-outs and to hydrogen embrittlement^{9,10}. The detrimental effect of hydrogen is due to its solubility behaviour. Hydrogen solubility in liquid steel is considerably higher than in solid steel. As a result, diatomic hydrogen is formed during cooling and solidification of the steel. The hydrogen gas creates pressure sites in the steel matrix, which may give rise to failure or surface defects. Though hydrogen pressure may build up at the inclusion-steel interface, we aim to investigate whether hydrogen dissolved in steel influences the formation and the shape of inclusions and whether hydrogen/water affects the separation of inclusions at the steel-slag interface. The research goals for hydrogen control are roughly divided in two items:

- The formation of inclusions in the liquid steel
- The separation of inclusions from the liquid steel.

The formation of inclusions in the liquid steel

Deoxidation of the liquid steel by the addition of a strong deoxidizer, such as aluminium, is the main source of inclusions. Various inclusion morphologies have been reported: clusters, dendrites, aggregates, small faceted particles, platelets and spherical inclusions¹¹⁻¹⁹. Clusters and aggregates contribute to most of the oxygen present in the steel (steel cleanliness)¹⁹. Clusters are typical for the deoxidation stage and are removed within about 15 minutes, while aggregates occur only after a few minutes after deoxidation and increase in size with holding time¹⁹. Since clusters are removed relatively fast from the steel bath, enhancement of cluster formation during deoxidation may result in lower total oxygen content of the steel (Figure 1). Therefore, control of inclusion morphology is expected to enable cleaner steel production.

The morphology of inclusions depends on the conditions during their formation and growth. The research goal is to look for a relationship between the cleanliness (the shape, the size and the number of inclusions) of the liquid steel and its hydrogen content. Adachi *et al.*²⁰ suggest that the presence of metastable alumina may be related to hydrogen in the steel. No description of the morphology of the inclusions is given. The effect of hydrogen content of the

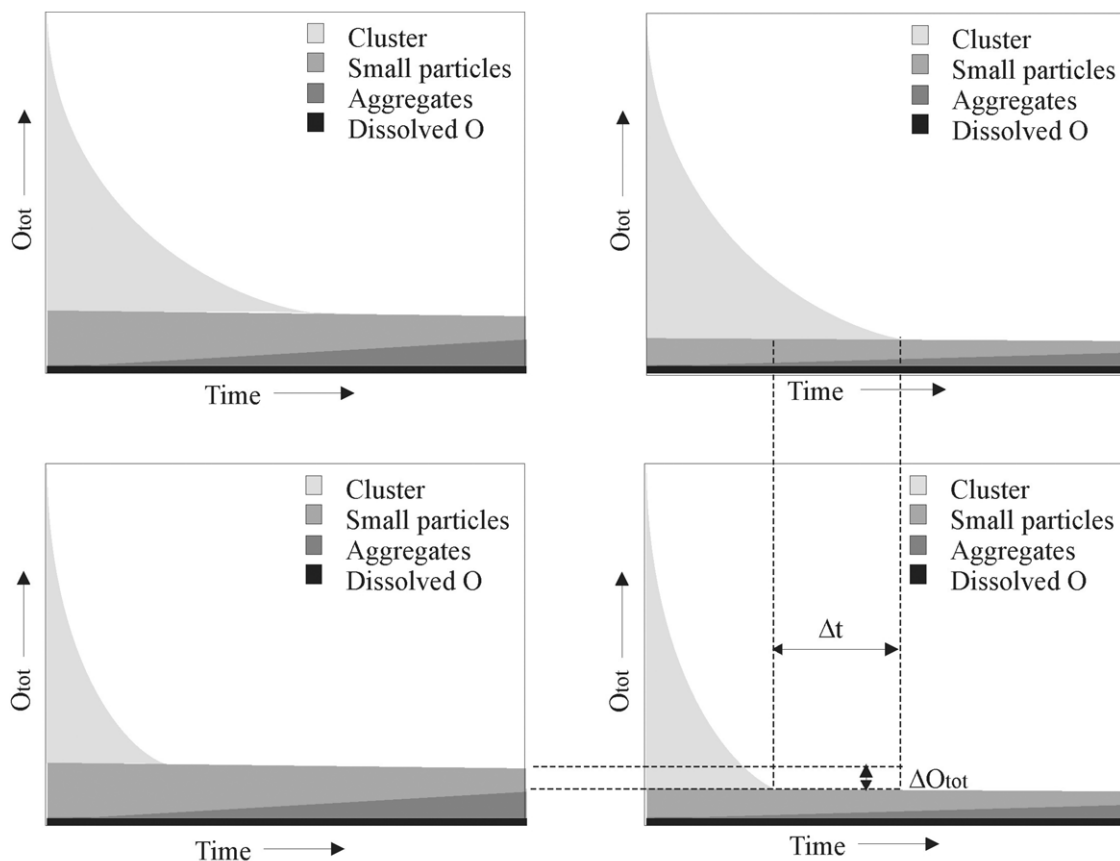


Figure 1. Evolution of the total oxygen content (O_{tot}) during ladle metallurgy. Initial state (upper left), increased fraction of clusters (upper right), increased rate of cluster removal (lower left) and increased fraction of clusters combined with high removal rate (lower right)

steel on the morphology of inclusions has never been investigated. If hydrogen influences the nucleation and growth of inclusions, it may affect the shape, size and number of inclusions in the steel. Control of the inclusion shape or its size may enable more efficient inclusion removal or avoid formation of large and detrimental particles. For instance, if the formation of irregular clusters can be promoted, this results in a more efficient removal of oxide inclusions, because clusters are easily and completely removed from the steel during ladle metallurgy and thus less oxygen is available for non-cluster (smaller) inclusions (Figure 1). By influencing the shape or the size of inclusions, we aim to introduce hydrogen control as a tool for inclusion engineering.

The separation of inclusions from the liquid steel

It is well known that hydrogen contents in steel above 7 ppm affect the heat transfer of mould powders and may cause surface defects (stickers) on the cast steel and increase the risk of break-outs during casting^{21–25}. Pontoire²⁵ concludes that the water content of the mould powder may not exceed 1.5% in order to prevent breakouts.

Hydrogen itself is not soluble in oxide melts. It interacts with oxygen, which gives rise to the formation of hydrate bonds. Commonly, one refers to the water content of oxide melts. Literature concerning the effect of water on oxide melts focuses on high silica melts, e.g. magmas and glasses, which may contain significant amounts of water. In these type of melts water significantly affects the viscosity because the viscosity is then not determined by strong cation-oxygen bonds, but by weak hydrogen bonds^{26,27}.

Commonly, the silica content of basic slag (ladle and tundish) is rather low or only a few per cent. A high slag viscosity is generally considered as disadvantageous because inclusions may not separate from the steel and dissolve more slowly and thus the probability of re-entrainment of inclusions into the steel is high.

Since the steel-slag interface plays a crucial role in the separation of inclusions from the steel, research on the influence of hydrogen or water on the slag properties, e.g. the viscosity or the heat transfer, is necessary. Only recently, *in situ* observation of the behaviour of inclusions at the steel or slag-steel interface has become possible by using confocal scanning laser microscopy (CSLM)^{28–32}.

Thermodynamic considerations

Steel melt

At low oxygen levels in steel no iron oxide is formed and thermodynamic equilibrium is established between water vapour and dissolved hydrogen and oxygen:

$$K_{H_2O} = \frac{a_H^2 \cdot a_O}{P_{H_2O}} \quad [1]$$

Figure 2 shows the relationship between dissolved oxygen and hydrogen content for different water vapour pressures. Hydrogen content in excess of 25 ppm is not reached because it requires hydrogen pressures above 1 atm. In dry conditions ($P_{H_2O}=0.003$ atm), the hydrogen content of the non-deoxidized steel is limited to 2–4 ppm. The maximum solubility of hydrogen in iron in the case of

dry and humid ($P_{H_2O}=0.06$ atm) climate conditions is obtained if the iron contains less than 10 ppm and 200 ppm dissolved oxygen, respectively. Therefore, steel is less vulnerable to hydrogen pickup when tapped at dry conditions than at humid conditions.

In practice, steel is deoxidized by addition of a strong deoxidizing alloy such as aluminium. After deoxidation, the oxygen activity of the steel is set by the activity of the deoxidizer and the solubility of hydrogen is not limited by the steel composition, i.e. maximum solubility exists. Thus detrimental hydrogen contents for casting (7–8 ppm) are feasible by thermodynamics and can be reached in all deoxidized steel grades. The reason that very high hydrogen contents do not occur frequently is that the steel is protected from the atmosphere by a slag. The slag additions are often stored and protected from humid conditions, such that the slag introduces minimal quantities of hydrogen to the steel.

In summary, liquid steel is not saturated with hydrogen at steelmaking conditions. Hence, hydrogen control based on the thermodynamic properties of the steel melt is not an option in industry.

Slag systems

The objectives of the slag are protection of the steel against atmospheric reoxidation, thermal insulation, and entrapment of inclusions from the steel. The slag is in contact with the atmosphere and, in particular, lime and magnesia react with the water vapour from the atmosphere. Though water absorption in the slag is of major concern to the slag product, the effect of water vapour pressure on the molten slag viscosity has not been considered so far. In order to get an idea of the amount of water that can be taken up by the slag, thermodynamic calculations have been carried out to determine the equilibrium at different slag compositions and at different water vapour pressures ($P_{H_2O}=0.06$ and 0.003 , 1873 K, 1 atm).

Figure 3 shows the isothermal sections of the systems

Al_2O_3 -CaO-MgO, Al_2O_3 -CaO-SiO₂ and CaO-MgO-SiO₂. The slag compositions are plotted as red spots. The water contents (in ppm) are given in blue and in grey at $P_{H_2O}=0.06$ and 0.003 , respectively. The hydrophylic character of CaO and MgO can easily be recognized from the values of the water contents. Basic slags are therefore most likely to show any influence of the water vapour pressure.

The question arises to what degree the water content affects the viscosity of the slag. In a CaO- Al_2O_3 slag, the aluminium atoms are tetrahedrally co-ordinated by oxygen atoms and as such a tetrahedral AlO_4 network is created in which the calcium atoms balance the atomic charge. The connection between two adjacent AlO_4 tetrahedra is broken by the addition of an H_2O molecule. At $P_{H_2O}=0.06$ the slag contains 458 ppm H_2O , which may break about 2 tetrahedral bonds out of 1 000. Therefore it is doubtful whether the viscosity is affected by water.

It must be remarked that the validity of the slag database (FACT-SLAGB) for hydrogen is unknown. So far, no data in literature have appeared concerning water vapour pressures during the steelmaking process. Also the viscosity of slag with a certain water content or at a defined water vapour pressure has not been reported. If the water content of the slag affects the slag viscosity, one may wonder whether the viscosity should be controlled by manipulating the water vapour pressure or by changing slightly the slag composition.

Rate of inclusion dissolution into a slag

IRSID developed a technique to investigate the rate of inclusion removal by the slag³³. The experimental technique consists of melting the top of a steel rod containing an oxide powder in an induction furnace (Figure 4). The steel rod diameter is 5 mm and the melted zone weight is typically 1.4 g. The amount of oxide powder added is around 1 mg. In the induction furnace, the oxide

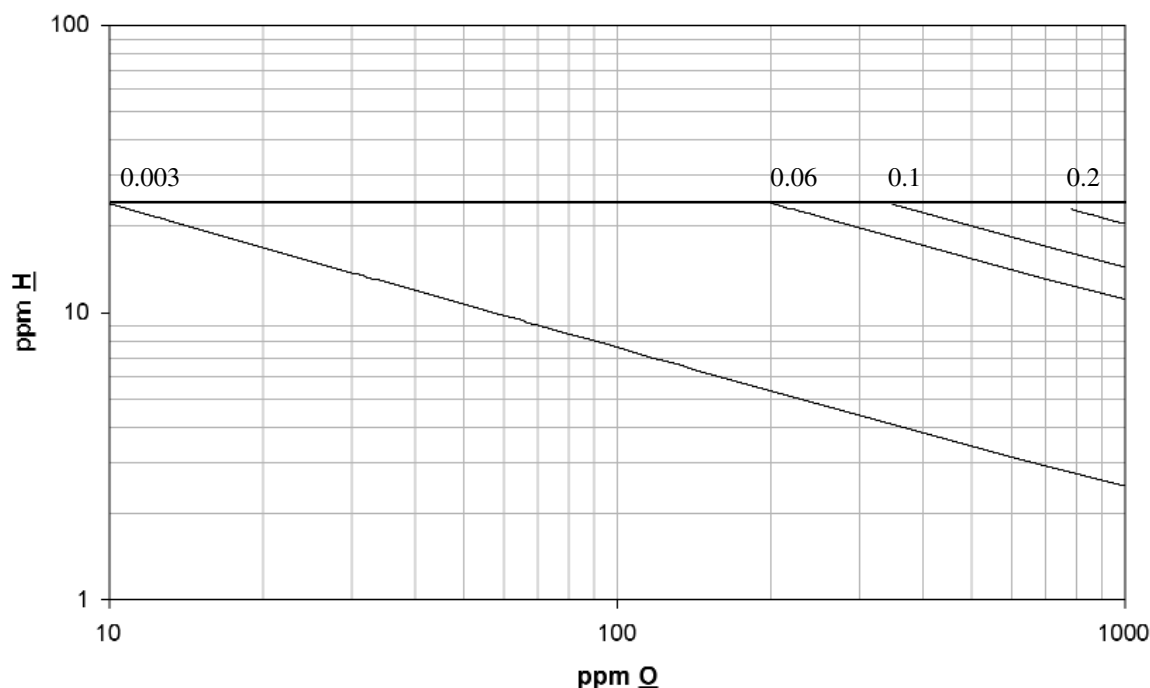


Figure 2. Hydrogen-oxygen equilibrium in iron for different water vapour pressures (1873 K, 1 atm)

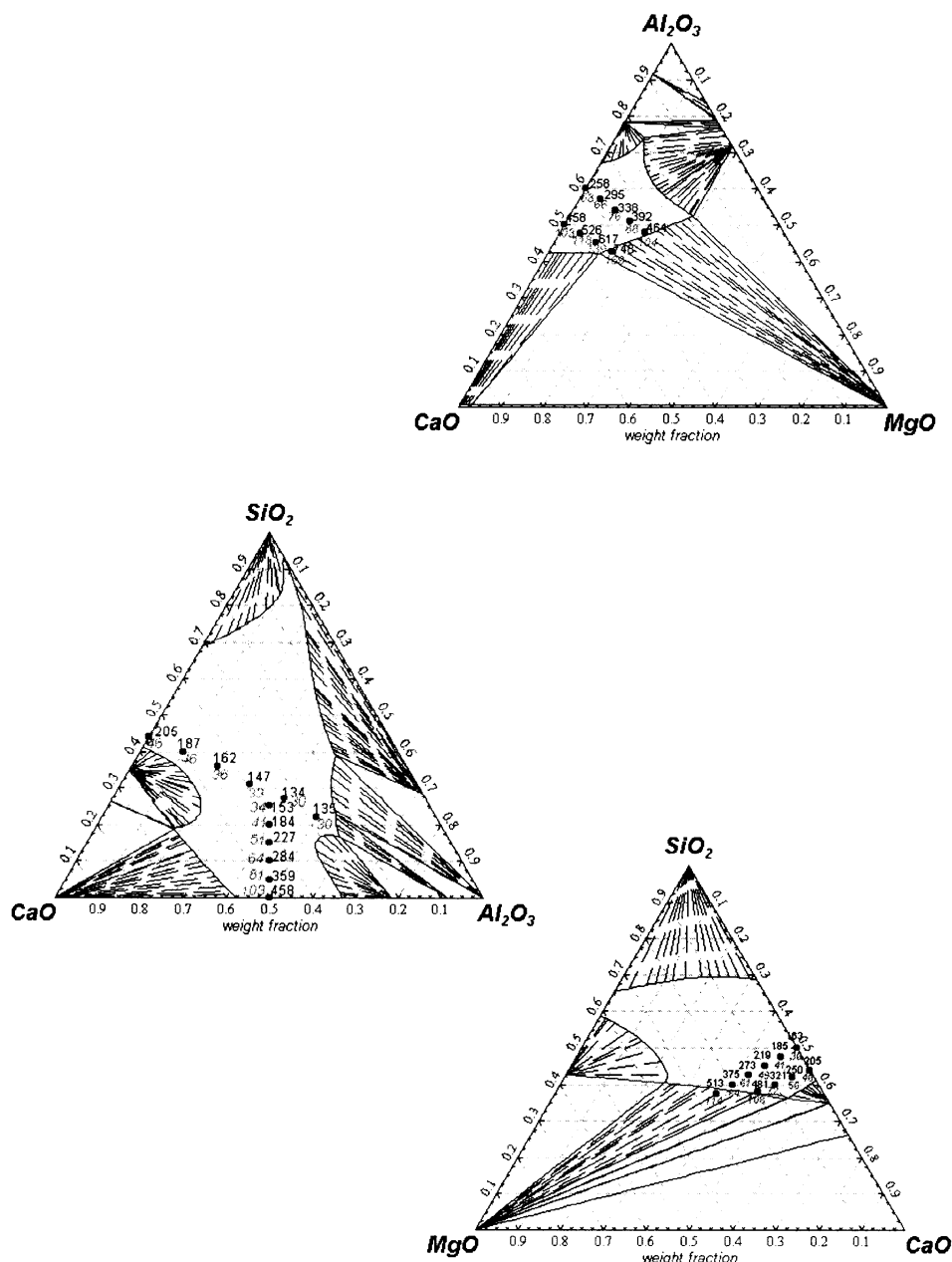


Figure 3. Isothermal sections of the systems Al_2O_3 -CaO-MgO, Al_2O_3 -CaO-SiO₂ and CaO-MgO-SiO₂. The slag compositions are plotted as spots. The water contents (in ppm) are given in black and in grey at $P_{\text{H}_2\text{O}}=0.06$ and 0.003, respectively

powder melts partially or entirely depending on its liquidus temperature and forms a slag droplet. The liquid metal drop remains at the top of the solid rod for a few minutes (3–6 min). Neither the steel nor the slag is in contact with any refractory material, so that mass transfer occurs only through the gas phase or the metal-slag interface. The atmosphere is Ar or Ar + various percentages H₂ (see below) with a gas flow of 1 l. min⁻¹. The steel used is an IF-Ti, whose composition is given in Table I. The LDSF slag used is an industrial powder. Its composition is given in Table II.

As the emissivities of oxide and liquid steel are different, the behaviour of the inclusion rafts and the slag droplet can be observed directly on the surface of the metal drop. The trials are recorded with a digital high-speed video camera, which allows for measuring the rate of entrapment by image analysis. The fusion temperature measured by a pyrometer is about 1530°C.

The surface and the length of contact arc between the inclusion raft and the slag droplet are measured by image analysis. The inclusion raft is progressively trapped by the

Table I
Steel composition (wt %)

Si	Al	Ti	Mn	P	C	Cr	Ni
0.037	0.037	0.057	0.120	0.011	0.002	0.021	0.09

Table II
Slag composition (wt %)

SiO ₂	Al ₂ O ₃	CaO	TiO ₂	MnO	MgO	Cr ₂ O ₃	P ₂ O ₅	Fe
1.95	42.26	51.33	2.32	<0.02	0.13	0.05	0.13	0.97

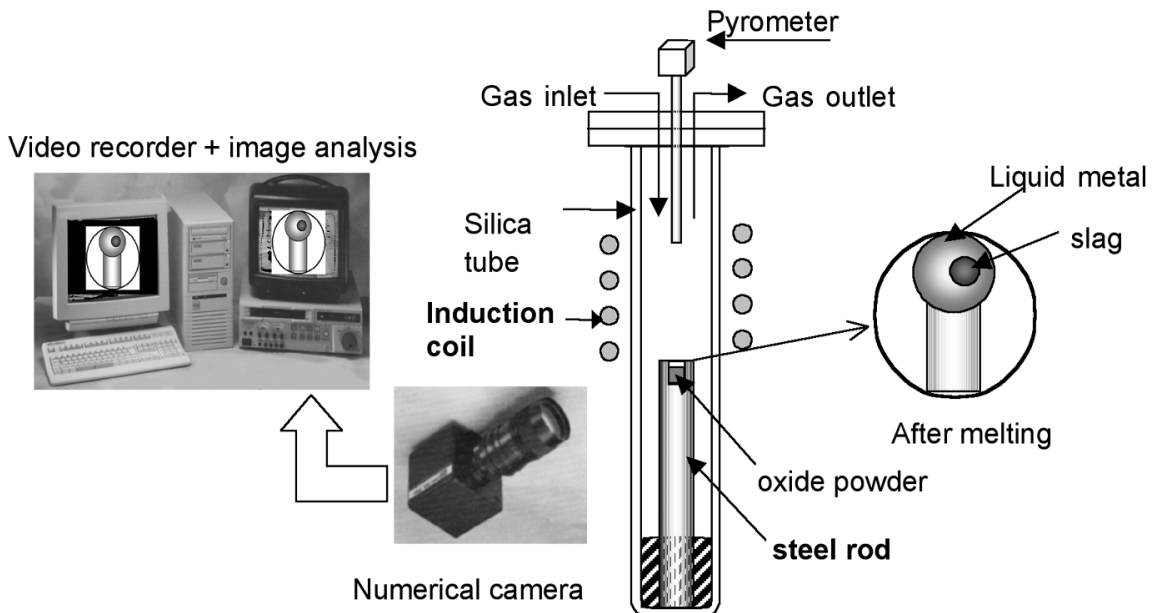


Figure 4. Experimental set-up of the inclusion entrapment experiment (IRSID)

slag droplet so that its surface S changes with time. The ratio of the trapped surface (ΔS to the length of the arc $l(t)$) is plotted versus time to measure the experimental entrapment rate V_{entr} :

$$V_{entr} = \frac{\Delta S}{l(t)\Delta t} \quad [2]$$

Although the experimental points are rather scattered, the slags' behaviour can clearly be distinguished from one another. The errors can be estimated by:

$$\delta V_{entr} / V_{entr} = \frac{\delta(\Delta S)}{\Delta S} + \frac{\delta l(t)}{l(t)} + \frac{\delta(\Delta t)}{\Delta t} \quad [3]$$

The images are recorded at 50 or 125 images per second and the time between two images is determined by the camera speed. The time error can be neglected compared to the surface and length measurements $\delta(\Delta t) = 0$. The errors on the surface and arc measurements are estimated to be respectively 10 and 15%. Thus, the calculated error of the entrapment rate due to the measurements is 18%. Experiments have been performed under four different gaseous atmospheres: pure Ar, Ar-0.5% H₂, Ar-5% H₂, Ar-20% H₂.

Pure Ar

Five trials have been performed and interpreted according to the procedure detailed here above. The results are presented in Figure 5. The entrapment rate is equal to 14 $\mu\text{m.s}^{-1}$.

Argon-hydrogen mixtures

For each atmosphere composition, five trials have been performed. Under this kind of gaseous mixture, slag has a more pronounced tendency to slip to the limit between the liquid steel droplet and the solid rod (Figure 6), which makes more difficult and less stable its contact with the inclusions rafts. Due to the hydrogen content of the gas, few inclusion rafts are formed and the rod rapidly becomes clean (Figure 7). Therefore, the results are more scattered than those obtained on pure Ar as shown on Figure 8.

The calculated entrapment rates are reported in Figure 8. The presence of hydrogen in the atmosphere seems to slow down the entrapment by the slag. If the difference between pure Ar and hydrogen bearing atmosphere appears to be well established, the difference of entrapment rates measured at different compositions of the H₂ bearing atmospheres is less clear because of the important scatter on the results.

Microscopy

The metallic droplets are investigated for the type of inclusions and the interface between the steel and the slag. Scanning Electron Microscopy (Philips XL30 FEG SEM equipped with EDAX energy dispersive spectrometer) of the oxide rafts indicates that at high hydrogen content, the oxide raft is built up by aggregates of small particles, while at low hydrogen contents the raft is formed by dendrite particles (Figure 9). Furthermore, the particles contain more titanium oxide at low hydrogen partial pressure. The difference in inclusion type might be explained by the availability of oxygen to react with the molten steel. The

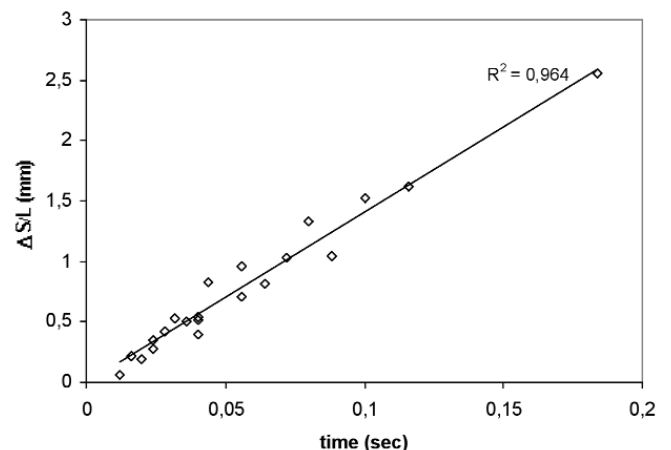


Figure 5. Experimental results obtained under pure Ar

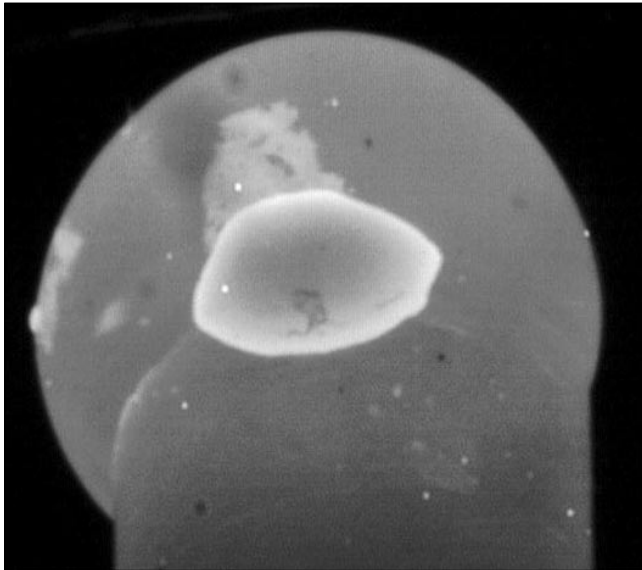


Figure 6. Uner Ar-20% H₂, the slag droplet has a tendency to slip towards the metallic droplet/rod interface

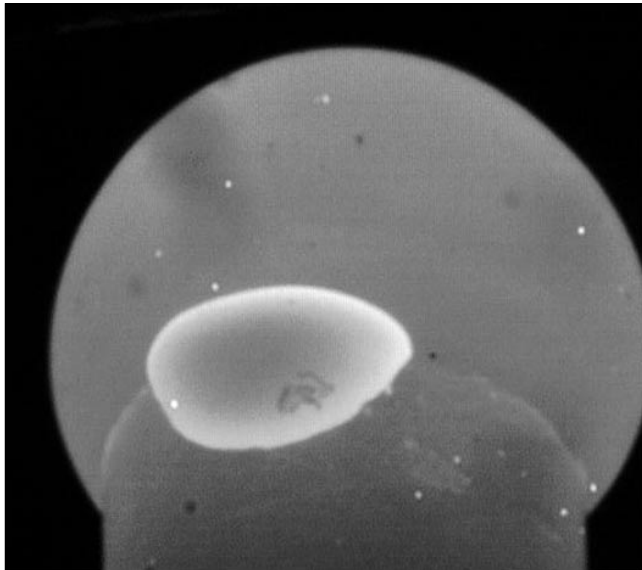
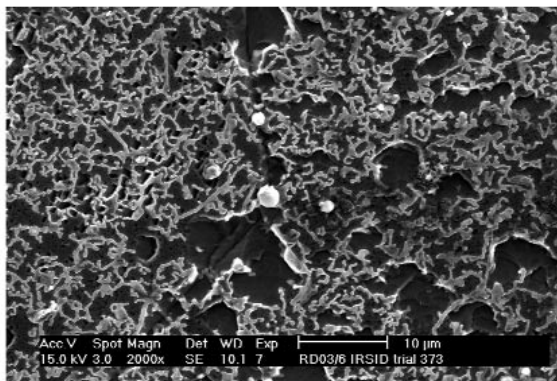


Figure 7. The rod is getting rapidly clean under a hydrogen bearing atmosphere (here Ar-20% H₂)



amount of oxygen in the system is supposed to be limited and due to the change of the steel rod between every experiment. High hydrogen content favours the formation of water vapour. Therefore, a part of the oxygen may be removed through the gas flow as water vapour, even before the steel starts to melt, i.e. the formation of oxide particles. Due to the lower oxygen activity in the hydrogen-rich atmosphere, there is, lower tendency for the formation of oxide inclusions. Nucleation time is extended, which results in more nuclei and as a result in less growth of the nuclei, i.e. formation of small particles is preferred above dendrite growth. The amount of titanium oxide formed may depend directly on the oxygen activity or on the lack of dissolved aluminium as the experiment proceeds.

Investigation of polished surfaces of the slag phase shows a homogeneous (glassy) phase, sometimes partially containing CaO·Al₂O₃ dendrites (Figure 10). No inclusions in the slag phase or along the slag-steel interface have been detected. The CaO·Al₂O₃ dendrites are supposed to be formed during cooling of the sample. The slag was not supersaturated with alumina during the experiment and therefore inclusion entrapment was not hindered. Wobbling of the droplet is supposed to give rise to the bulging steel-slag interface, which was often observed. Measurement of the wetting angle between steel and slag as a function of the partial hydrogen pressure was not carried out because a cross-section along the centre of the slag droplet is required.

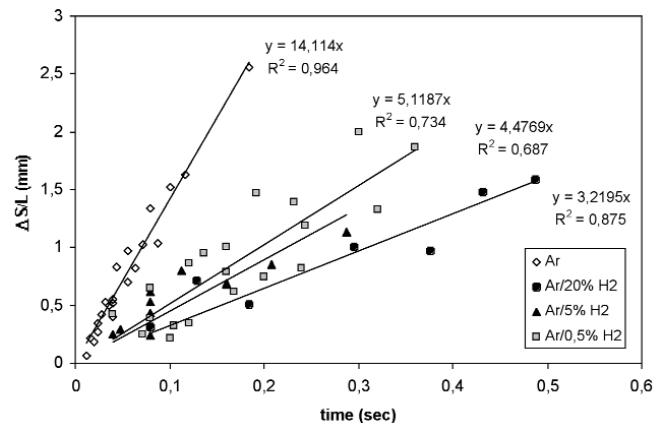


Figure 8. results obtained under pure Ar and Ar-H₂ atmosphere

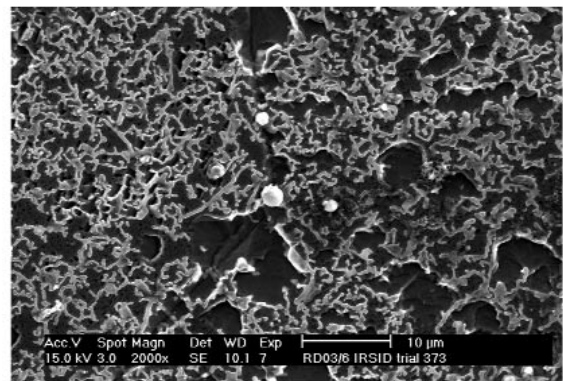


Figure 9. Morphology of oxide rafts consists of dendrite-like particles in Ar atmosphere and agglomerated particles form the raft in 20% H₂-Ar atmosphere

Industrial measurements

Data acquisition

At least one hydrogen measurement (HydriS, Heraeus Electro-Nite) and one steel pin sample (TOS, Heraeus Electro-Nite) was taken for every heat. Data acquisition was carried out at two steel plants. Though some reoxidation of the steel in the tundish may occur, sampling at the stirring station may not be relevant because inclusions separation still continues, while the ladle is frequently not accessible just before casting. Sampling occurred when half of the ladle was cast and its location was constant. Multiple sampling series of certain heats in the tundish at Plant A confirmed that hydrogen content does not change significantly, even when a new tundish was taken into operation. The variation of total oxygen content was frequently significant, including extremes with more than 50 ppm difference.

The results obtained from Plant B are plotted in Figure 11 and are divided into the four major steel grade groups, i.e. low carbon aluminium killed steel (KZ), medium carbon aluminium killed steel (KH), low carbon silicon-aluminium killed steel (L) and ultra-low carbon steel (ULC). The hydrogen content is always below 5 ppm. Since a small correlation between hydrogen content and total oxygen content may exist, additional measurements are carried out. Both the hydrogen content and the total oxygen content

could not be correlated to manganese addition, aluminium addition, scrap addition, carbon content, lime content of the ladle slag, dissolved oxygen content prior to deoxidation, aluminium loss, holding time of the ladle, or stirring conditions.

At Plant A the hydrogen contents vary significantly and reach values up to 10 ppm (Figure 12). The high hydrogen contents are due to bottom oxygen blowing in the converter, which requires hydrocarbon gases as a cooling medium for the tuyeres. Since no information about the steel grade and the process has been supplied, no statistical evaluation of the results is carried out. The data of Plant A do not confirm any correlation between the hydrogen content of the steel and its total oxygen content. On the contrary, it can be stated that high hydrogen content does certainly not result in high total oxygen content. Thus the presence of hydrogen seems not to give rise to lower cleanliness with respect to inclusions. In addition, no data has been obtained that plots in the high- O_{tot} -high-hydrogen or the low- O_{tot} -low-hydrogen corners. The question arises whether this is due to the limited data points or whether hydrogen does affect the steel cleanliness or vice versa.

Inclusions

For each plant the following TOS samples from non-degassed grades have been selected for inclusion investigation: (1) five samples with the highest hydrogen

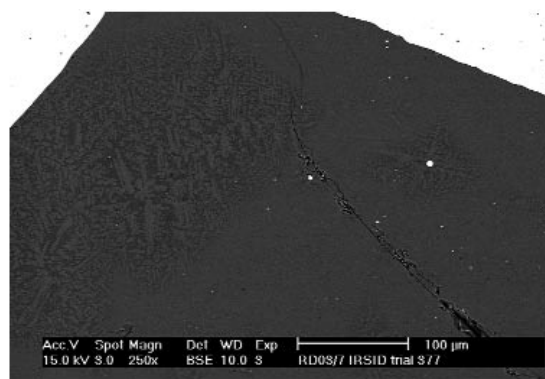
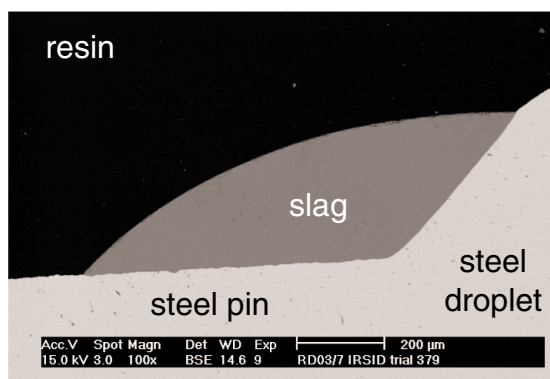


Figure 10. Cross-section along the slag droplet, the steel droplet and the solid steel pin (left). The slag is partially crystallized. Notice the white steel droplet in the right micrograph, which acts as a nucleation site for $\text{CaO}\cdot\text{Al}_2\text{O}_3$ dendrites (right)

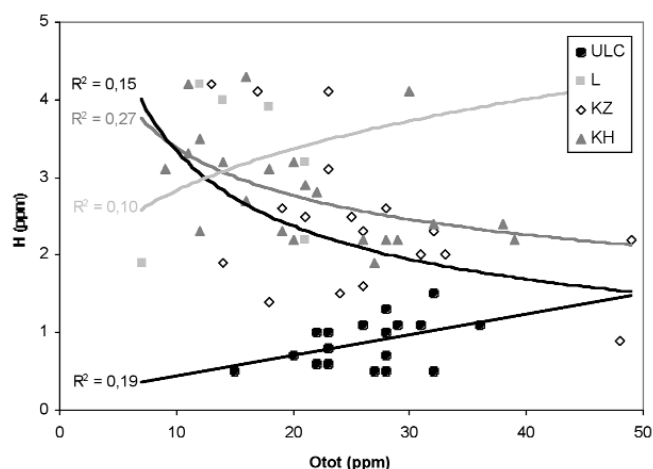


Figure 11. Plot of hydrogen content and total oxygen content of heats sampled in the tundishes at Plant B

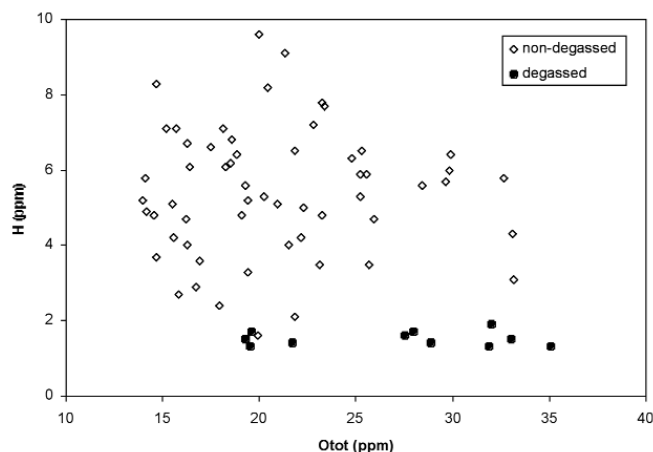


Figure 12. Plot of hydrogen content and total oxygen content of heats sampled in the tundishes at Plant A

content, (2) five samples with the lowest hydrogen content, (3) five samples with highest total oxygen content and (4) five samples with the lowest total oxygen content. The inclusions were extracted by dissolving the steel in hot hydrochloric acid, followed by filtration through a porous membrane. The membrane with inclusions was investigated under the SEM. The size and shape of the big inclusions, e.g. clusters, aggregates, and dendrites, were recorded (at least 20 particles per sample). Aggregates appeared to be present in sufficient degree, while clusters and dendrites occurred only sporadically (Figure 13). Although a correlation between the size of big inclusions and the total oxygen content was supposed, because the big inclusions represent a large amount of the volume of oxide, this was not confirmed by the results obtained at the two steel plants (Figure 14). Whether the hydrogen content influences the size of aggregates is debatable (Figure 14).

Apart from the big inclusions, the very small spherical inclusions have also been considered. It has been proven that the small spherical alumina particles are formed during sampling of the liquid steel, i.e. segregation of oxygen during solidification³⁴. Since sampling is equivalent for all heats, differences in particle size may be related to the steel composition, including hydrogen content. No significant size difference has been recognized so far (Figure 15).

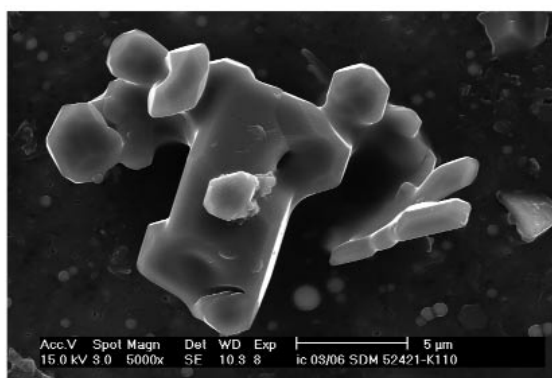


Figure 13. Inclusions from tundish samples, aggregate (left) and dendritic growth on polyhedral (right)

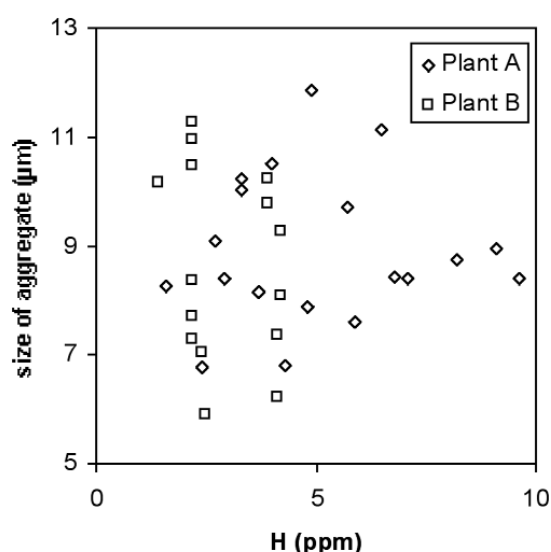
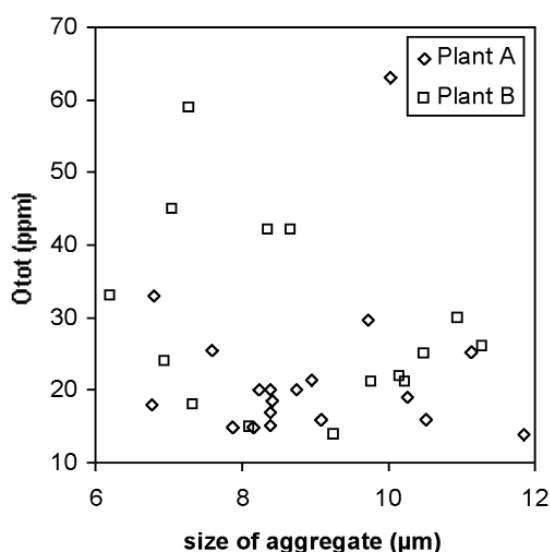


Figure 14. Average size of aggregate-type inclusions in the tundishes of Plant A and Plant B in function of the total oxygen content of the steel (left) and hydrogen content versus average size of aggregates in tundish (right)

Conclusions

So far no evidence has been found that hydrogen dissolved in steel may affect the steel cleanliness. The influence of hydrogen or water vapour on the slag properties is supposed to be limited from thermodynamic considerations. The different oxide inclusion rafts in the case of the IRSID experiments is supposed to be due to availability of oxygen during the experiments.

Acknowledgements

This research has been financed by the Flemish Institute for Technology Innovation: project 020365.

References

1. MOTLAGH, M. Improvements in the DH Vacuum Degassing Efficiency at the Commonwealth Steel Company. *Ironmaker Steelmaker*, vol. 20, no. 2. 1993. pp. 41–53.
2. DOR, PH., CARRIER, B., NADIF, M., and GATELLIER, C. Influence du laitiers sur la déshydrogénation de l'acier sous vide. *Rev. Metallurgie*, April. 1988. pp. 307–316.

3. BANNENBERG, N., BERGMANN, B., and GAYE, H. Combined decrease of sulphur, nitrogen, hydrogen and total oxygen in only one secondary steelmaking operation. *Steel Research*, vol. 63, no. 10. 1992. pp. 431–437.
4. BANNENBERG, N. Wechselwirkungen zwischen Feuerfestmaterial und Stahl und deren Einfluß auf den Reinheitsgrad des Stahls. *Stahl u. Eisen*, vol. 115, no. 10. 1995. pp. 75–82.
5. HAASTERT, H.P. Entwicklungsrichtungen der Sekundärmetallurgie, im besonderen das RH-Verfahren zur Vakuumbehandlung. *Stahl u. Eisen*, vol. 111, no. 3. 1991. pp. 103–109.
6. BANNENBERG, N., BRUCKHAUS, R., LACHMUND, H., and SCHMITT, F.J. Sekundärmetallurgische Behandlung für die Erzeugung von Grobblechstählen. *Stahl u. Eisen*, vol. 118, no. 7. 1998. pp. 33–36.
7. VOLLRATH, K. Symposium über Anwendungen der Vakuummetallurgie. *Stahl u. Eisen*, vol. 119, no. 12. 1999. pp. 93–95.
8. KLEIMT, B., KOEHLE, S., and JUNGREITHMEIER, A. Dynamic model for on-line observation of the current process state during RH degassing. *Steel Research*, vol. 72, no. 9. 2001. pp. 337–345.
9. MEYER, W., HOCHÖRTLER, J., ENGHOLM, M., JÖRGENSEN, D., and SANDBERG, A. Experiences with on-line determination of hydrogen content in ladle refining of tool steels. *Proceedings of the 6th Int. Conf. on Refining Processes*, Luleå, Sweden. MEFOS-Jernkontoret, 1992. Part II, pp. 277–302.
10. LACHMUND, H. SCHWINN, V., and JUNGBLUT, H.A. Heavy plate production: demand on hydrogen control. *Ironmaking and Steelmaking*, vol. 27, no. 5. 2000. pp. 381–386.
11. STEINMETZ, E. and LINDENBERG, H-U. Morphology of inclusions at aluminum deoxidation. *Arch. Eisenhüttenwes.*, vol. 47, no. 4. 1976. pp. 199–204.
12. STEINMETZ, E., LINDENBERG, H-U., MÖRSDORF, W., and HAMMERSCHMID, P. Shapes and formation of aluminum oxides in raw ingots and continuously cast slabs. *Stahl u. Eisen*, vol. 97, no. 23. 1977. pp. 1154–1159.
13. STEINMETZ, E., LINDENBERG, H-U., MÖRSDORF, W., and HAMMERSCHMID, P. Growth shapes of aluminum oxides in steels. *Arch. Eisenhüttenwes.*, vol. 48, no. 11. 1977. pp. 569–574.
14. BRAUN, T.B., ELLIOTT, J.F., and FLEMINGS, M.C. The Clustering of Alumina Inclusions. *Met. Trans. B*, vol. 10B. 1979. pp. 171–184.

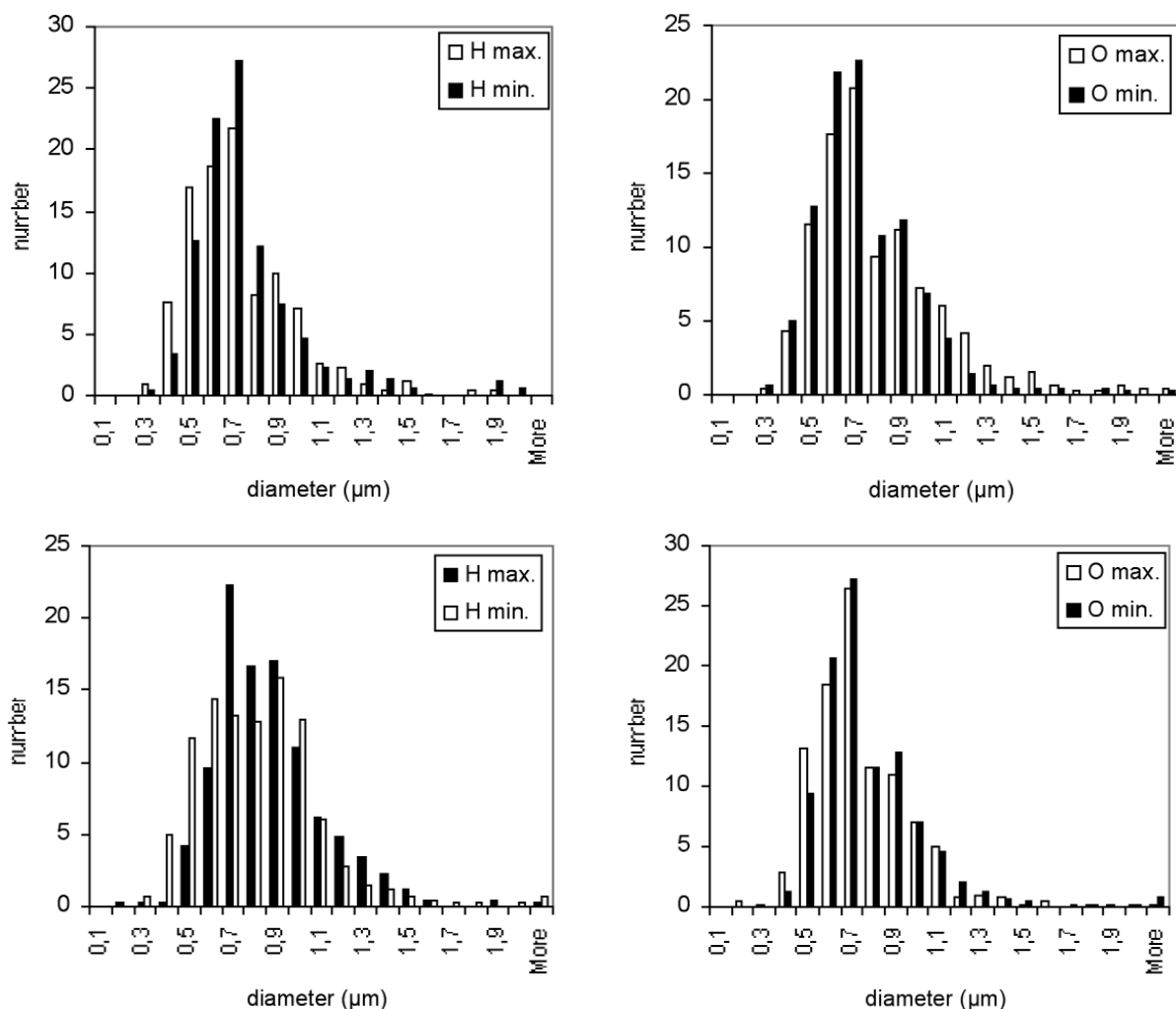


Figure 15. Size of spherical alumina particles in the selected TOS samples

15. STEINMETZ, E. and LINDENBERG, H.-U. Hammerschmid P., and GLITSCHER, W. Oxidbildung in aluminiumdesoxidierten Stahlschmelzen bei Rückoxidations-Vorgängen. *Stahl u. Eisen*, vol. 103, no. 11. 1983. pp. 539–545.
16. STEINMETZ, E. and ANDREAE, C. Einfluß des sauerstoffs auf die Ausbildung von Aluminiumoxiden in Eischmelzen. *Steel Research*, vol. 62, no. 2. 1991. pp. 54–59.
17. TIEKINK, W., PIETERS, A., and HEKKEMA, J. Al_2O_3 in Steel: Morphology Dependent on Treatment. *Ironmaker Steelmaker*, vol. 21, July. 1994. pp. 39–41.
18. DEKKERS, R., BLANPAIN, B., WOLLANTS, P., HAERS, F., VERCRUYSEN, C., and PEETERS, L. Evolution of non-metallic inclusions in liquid low alloyed low carbon steels. *Proceedings of the EPD Congress of the TMS-conference*, San Diego, USA. Mishra, B. (ed.). Pittsburgh. TMS, 1999. pp. 269–276.
19. DEKKERS, R., BLANPAIN, B., WOLLANTS, P., HAERS, F., VERCRUYSEN, C., and GOMMERS, B. Non-metallic inclusions in aluminium killed steels. *Ironmaker Steelmaker*, vol. 29, June. 2002. pp. 161–171.
20. ADACHI, A., IWAMOTO, N., and UEDA, M. Consideration on the deoxidation mechanism of steel with metallic aluminium. *Trans ISIJ*, vol. 6. 1966. pp. 24–30.
21. IMAI, T. SUDO, F. OKMIYA, S., and TAKE, H. The effect of high-hydrogen content steel on CC operation and countermeasures in the K-BOP process. *13th Conf. of OEM/Q-BOP*, Rottach-Egern. 1986.
22. ZASOWSKI, P.J., and SOSINSKY, J. Control of heat removal in the continuous casting mould. *Proc. 9th Process Technology, 49th Ironmaking and 73rd Steelmaking Conf.*, Detroit, USA. ISI, 1989. pp. 393–400.
23. PONTOIRE, J.N., LEFEBVRE, C., FRISCOURT, J.L., and LOPEZ, J.P. Contrôle de la teneur en H_2O des poudres de coulée continue. *Rev. Metallurgie*, no. 10. 1996. pp. 1237–1240.
24. MCKAY, S. Investigation of the influence of hydrogen in liquid steel on the heat transfer in the continuous casting mould. *Hydrogen in steel: Processing and product requirements*, London, UK. The Institute of Materials, 1999.
25. PONTOIRE, J.N., RADOT, J.P., DELVAUX, V., and DHAUSSY, E. Coulée continue d'acier non dégazé: detection de l'hydrogène dans le film de laitier infiltré. *Rev. Metallurgie*, no. 1. 2000. pp. 35–41.
26. WHITTINGTON, A., RICHET, P., LINARD Y., and HOLTZ, F. The viscosity of hydrous phonolites and trachytes. *Chem. Geology*, vol. 174. 2001. pp. 209–223.
27. RICHET, P., LEJEUNE, A.-M., HOLTZ F., and ROUX, J. Water and the viscosity of andesite melts. *Chem. Geology*, vol. 128. 1996. pp. 185–197.
28. YIN, H., SHIBATA, H., EMI, T., and SUZUKI, M. 'In situ' Observation of Collision, Agglomeration and Cluster Formation of Alumina Particles on Molten Steel Surface. *ISIJ Int.*, vol. 37, no. 10. 1997. pp. 936–945.
29. YIN, H., SHIBATA, H., EMI, T., and SUZUKI, M. Characteristics of Agglomeration of Various Inclusion Particles on Molten Steel Surface. *ISIJ Int.*, vol. 37, no. 10. 1997. pp. 946–955.
30. TSE, C., LEE, S.H., SRIDHAR, S., and CRAMB, A.W. In situ observations relevant to clean steel: dissolution of alumina particles in slags. *Proceedings of the 83rd Steelmaking Conf.* 2000. pp. 219–229.
31. SRIDHAR, S. and CRAMB, A.W. Kinetics of Al_2O_3 dissolution in $CaO-MgO-SiO_2-Al_2O_3$ slags: in situ observations and analysis. *Metallurgical and Materials Transactions B*, vol. 31B, no. 4. 2000. pp. 406–410.
32. LEE, S.H., TSE, C., MISRA, P., CHEVRIER, V., ORLLING, C., SRIDHAR, S., and CRAMB, A.W. Separation and dissolution of Al_2O_3 inclusions at slag/metal interfaces. *Proc. of the 6th Int. Conf. on Molten Slags, Fluxes and Salts*, Stockholm-Sweden and Helsinki-Finland. S. Seetharaman and Du Sichen (eds.) KTH, Stockholm, 2000. pdf128.
33. ROCABOIS, P., SAINT RAYMOND, H., and GATELLIER, C. Physical and theoretical modelling of alumina inclusions entrapment by slags. ICS 2001, *Proc. 2nd Int. Cong. On the Science & Technology of Steelmaking*, Swansea, UK. London. IOM Communications, 2001.
34. DEKKERS, R. Non-metallic inclusions in liquid steel. Ph.D. Thesis, K.U.Leuven, 2002. Acco, Leuven, Belgium.